

Minimizing Communication Delay in RFID-based Wireless Rechargeable Sensor Networks

Yuanchao Shu*, Peng Cheng*, Yu Gu[†], Jiming Chen* and Tian He[‡]

*State Key Laboratory of Industrial Control Technology, Zhejiang University, China

[†] Singapore University of Technology and Design, Singapore

[‡] Dept. of Computer Science and Engineering, University of Minnesota, USA

Abstract—Integrated with low-power micro-controllers and sensors, RFID-based wireless rechargeable sensor node is a very promising platform for applications such as inventory management, supply chain monitoring etc. Among other major research challenges, one of the most essential problems in such wireless rechargeable sensor networks is how to minimize the communication delay among RFID readers and RFID-based rechargeable nodes. While the existing works have mostly focused on the collision avoidance among RFID-based nodes, in this work we study an orthogonal approach which focuses on how to optimally plan the movement of the reader so as to minimize the communication delay in the network. To solve this problem, we introduce both an optimal solution for the linear reader movement pattern and an approximation solution for the generic two-dimensional reader move pattern with a provable approximation ratio. In addition, we also provide a solution for guaranteeing the quality of communication while minimizing the communication delay. We verify our observations through testbed experiments and extensively evaluate our design by both emulations and large-scale simulations. The results show our design can effectively reduce communication delay in wireless rechargeable sensor networks when compared with baseline solutions.

I. INTRODUCTION

RFID-based wireless rechargeable sensor network (WRSN) is an emerging technology in which sensing and computational abilities are integrated to traditional RFID tags. Different from traditional sensor nodes which are powered by batteries, RFID-based wireless rechargeable sensor nodes gather their energy from transmissions of nearby RFID readers, and return sensory data to reader. Given their very small form factors and capabilities to sense the surrounding environments, RFID-based WRSN provides a very promising platform for applications such as warehouse inventory management [5], [17], supply chain monitoring [2], authentication [23], passive asset tracking [3] etc.

For a typical warehouse inventory monitoring application, wireless rechargeable sensor nodes are attached to various containers or individual products for sensing and monitoring vital product statuses such as temperature, humidity and vibration. To obtain the sensory data measured by wireless rechargeable sensor nodes, an RFID reader is normally deployed and can move around to communicate with all wireless rechargeable sensor nodes [1]. However, as wireless rechargeable sensor nodes are powered by the RFID readers and have little energy storage capacity, only when they are within the communication range of the RFID reader, they can perform their communication tasks [20]. So in order to minimize the total time duration

for the RFID reader to obtain the sensory information from all wireless rechargeable sensor nodes, intuitively, we should have the RFID reader cover as many sensor nodes as possible. On the other hand, as the number of sensor nodes within the communication range of an RFID reader increases, the collisions among sensor nodes also increase, which lead to a larger communication delay [8] [25].

In this work, instead of designing solutions for reducing collisions among sensor nodes, we study an orthogonal approach and focus on how to optimally plan the movement of the RFID reader, so as to minimize the communication delay of obtaining sensory data from all RFID-based wireless rechargeable sensor nodes. Rather than designing new protocols from scratch, our solutions exploit the fundamental relationship between the total communication delay and the number of wireless rechargeable sensor nodes within the communication range of an RFID reader. Based on this observation, we introduce novel solutions for determining the optimal movement pattern of the RFID reader along the fixed linear trajectory and generic two-dimensional space. Specifically, the major intellectual contributions of this work are as follows:

- To the best of our knowledge, this is the first try in minimizing communication delay based on RFID reader movement trajectories in RFID-based WRSN.
- We identify the fundamental relationship between the communication delay and the number of sensor nodes within the communication range of an RFID reader, through both mathematical analysis and empirical experiments.
- We introduce a novel and optimal solution for minimizing communication delay when RFID reader moves along a linear trajectory by transforming this problem to a shortest path problem, and also introduce sub-optimal solutions for minimizing communication delay when RFID reader can move in a two-dimensional space with a provable performance approximation ratio.
- We investigate the problem of how to guarantee the quality of communication through theoretical analysis, and validate the effectiveness of our design by extensive testbed experiments and large-scale simulations.

The remainder of this paper is organized as follows. We firstly introduce some preliminary knowledge of communication delay both for passive RFID and RFID-based wireless rechargeable sensor systems in Section II. After that, we describe the problem definitions of communication delay minimization and provide solutions with both linear and two-dimensional reader movements in Section III and Section IV,

respectively. Further discussions of quality of communication are presented in Section V. We evaluate our algorithms in Section VI and discuss related work in Section VII. Finally, we conclude in Section VIII.

II. COMMUNICATION DELAY IN WIRELESS RECHARGEABLE SENSOR NETWORKS

Firstly in this section, we describe communication process and examine delay characteristics of RFID-based WRSN. Based on that, we propose general delay minimizing algorithms in Section III and Section IV.

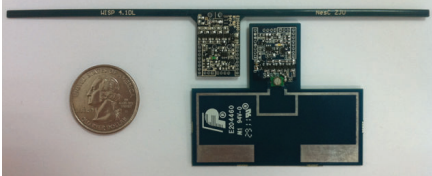


Figure 1. Two Types of WISP Nodes

Without loss of generality, we use Wireless Identification Sensing Platform (WISP) as a representing RFID-based wireless rechargeable sensor node [20] in this work. WISP is a fully-passive Ultra High Frequency (UHF) RFID tag that integrates a processor and several low-power sensors such as accelerometer and temperature sensors. We redesign the WISP on the basis of Intel's original model. Figure 1 shows two WISP nodes we made with different shapes of antenna. Through its antenna, a WISP node harvests energy from signals of nearby standard UHF RFID readers for both communication and powering other components of the WISP node.

WISP implements Electronic Product Code (EPC) Class 1 Generation 2 (C1G2) [11] communication protocol which is based on the Dynamic Framed Slotted ALOHA (DFSA) [21] and widely used in existing passive RFID systems. In following sections, we first describe DFSA protocol in detail and then discuss the communication delay between WISP nodes and the RFID reader through both theoretical analysis and empirical testbed experiments.

A. Dynamic Framed Slotted ALOHA Protocol

DFSA inherits many control commands that a reader can select to control the communication process between itself and RFID tags. Different from Framed Slotted ALOHA (FSA), in DFSA each frame has a variable number of slots. The frame size in DFSA is commonly denoted by N and the number of tags is denoted by n . At the beginning of one frame in DFSA, the reader broadcasts a *SELECT* command with a value of N , which indicates that the entire frame is divided into N slots. After receiving the *SELECT* command, a tag randomly chooses a slot RN between 1 and N that it plans to reply to the reader. After this initialization process, the reader sequentially broadcasts a *QUERY* command for each slot within a frame and each tag replies to the reader at RN slot it chosen before.

Due to the randomness of choosing reply slot among tags, empty slot, collision slot and successful slot all exist within a frame. In DFSA, the allocation of tags to slots within a frame belongs to the class of occupancy problems which are well-studied in probability theory and statistics [29]. Given the

frame size N and the number of tags n , the probability that x tags are allocated to one specific slot is binomially distributed as $P_x = \binom{n}{x} (\frac{1}{N})^x (1 - \frac{1}{N})^{(n-x)}$.

Therefore, using linearity of expectation, the expected number of slots with occupancy number x is given by $N_x = N \binom{n}{x} (\frac{1}{N})^x (1 - \frac{1}{N})^{(n-x)}$. Consequently, the expected number of successful slots N_1 , empty slots N_0 and collision slots N_c can be written as $N_1 = \binom{n}{1} (1 - \frac{1}{N})^{(n-1)}$, $N_0 = N (1 - \frac{1}{N})^n$ and $N_c = N - N_1 - N_0$.

If any collision slot exists within one frame, the reader will start a new frame and attempt to communicate with tags that are collided in the previous frame. The process continues until there is no collision detected within a frame. We term the whole process for a reader to communicate with all tags within its communication range a *communication round*.

B. Communication Patterns in RFID-based WRSN

In general, two different types of communication patterns exist for RFID-based wireless rechargeable sensor networks.

- **Multiple-Reply Pattern:** Like traditional RFID tags, wireless rechargeable sensor nodes such as WISP has the capability to reply the reader's query for multiple times as long as it is located within reader's communication range. Under the multiple-reply pattern, a node will only keep silent for one communication round of reader-tag communication after its successful communication with the reader. In the subsequent rounds, the node will become active again and contend to exchange data with the reader for each round [11]. Unlike RFID tags which only exchange its static identification information with the reader, wireless rechargeable sensor nodes are able to feedback dynamic sensory data and task outputs. The multi-reply pattern is essential for many wireless rechargeable sensor networks applications such as real-time monitoring.
- **Single-Reply Pattern:** Under the single-reply pattern, a tag may keep silent for multiple communication rounds after its successful communication with the reader in the first round. This communication pattern is unique to the RFID-based WRSN as with computational capabilities, a tag itself may use the feedback from the reader (e.g., ACK) to decide whether or not to communicate with the reader and avoids unnecessary communication collisions.

Considering wide implementations and adoptions of the multiple-reply communication pattern and its functionalities in the wireless rechargeable sensor networks, we primarily focus on the multiple-reply communication pattern in this paper. In section V, we will also discuss how to extend our solutions from the multiple-reply pattern to the single-reply pattern.

C. Reader-Tag Communication Delays

Firstly in this section, we simulate communication delay of multiple tags with both FSA and DFSA with different frame size selection mechanisms. Although the actual number of tags is unknown in many practical systems, it can be efficiently estimated using N_0 , N_1 and N_c [16] [25]. In this simulation, frame size in Figure 2(a) is fixed to 16 whereas in Figure 2(b), frame size is updated by the equation $N = N_1 + 2N_c$, where

N_1 and N_c are the number of successful and collided slots in the previous frame respectively [25].

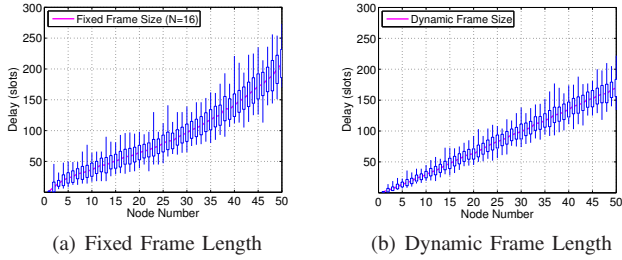


Figure 2. Simulated Communication Delay with Multiple Tags

From Figure 2, it can be found that communication delay grows with the number of tags and variances of communication delays are relatively small. Consequently we can see there is a direct mapping between the number of nodes and the expected reader-tag communication delays. Existing works also validate this observation using various theoretical methods [25].

To empirically study the communication delay of RFID-based wireless rechargeable sensor nodes, we also measured the actual communication delays for WISPs on our testbed. EPC C1G2 protocol is implemented in the off-the-shelf RFID reader whereas low-level behavior such as the adaptation of frame size is not revealed to the users. During the experiment, we place several WISPs in front of the antenna of a reader, and perform reader-tag communications in multiple rounds as we increase the number of nodes from 1 to 6. Reader retrieves 1000 sensory readings from WISPs. Experiments of WISP nodes and tags are conducted under the same condition and we repeat each test for 6 times.

In experiments, we find delay for WISP nodes grows when the number of nodes increases. From Table I, we find delay variances in real experiments are also small compared with the total delay, which is consistent with our simulation results. Consequently, despite of little information of the detailed low-level protocol, we can conclude that the reader-tag communication delay is highly correlated to the number of nodes within the communication range.

Table I. COMMUNICATION DELAY VARIANCE OF WISP NODES

Node Number	1	2	3	4	5	6
Delay Variation (%)	5.48	7.69	8.32	8.95	8.76	8.25

In the following sections, we exploit this observation on the reader-tag communication delay and introduce solutions for optimal reader movement planning both under constrained linear movement pattern and generic two-dimensional movement pattern. Solutions proposed in the rest of the paper are independent of any type of RFID communication model as long as the delay mapping is available (e.g., the expected delay curve). Since delay variance existed in practical scenarios, we also introduce solutions to guarantee the percentage of successful reader-tag communications in Section V-A.

III. MINIMIZING COMMUNICATION DELAY WITH LINEAR READER MOVEMENT

In the previous section, we have both analytically and experimentally investigated the relationship between the communication delay and the number of wireless rechargeable

sensor nodes. By utilizing such delay information, in this section, we introduce an optimal solution for minimizing total communication delay with linear reader movement trajectory.

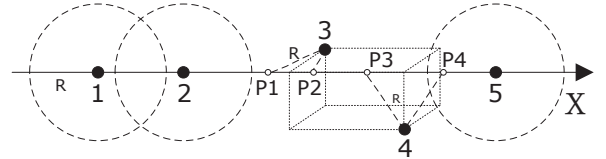


Figure 3. Linear Distribution of WISP Nodes

Linear reader movement exists in warehouse inventory management, supply chain monitoring and other scenarios where one reader moves along single track and stops at several locations (from infinity candidates) to communicate with nodes in vicinity [28]. Specifically, to communicate with a linear deployment of nodes such as node 1, 2, 5 shown in Figure 3, a reader moves from one end of the deployment to the other end of the deployment. During such linear movement, the reader stops at several locations and queries sensory readings at individual nodes. Even for nodes deployed in a 3D space, they can be easily mapped onto a linear line with linear reader moving trajectories. For example as shown in Figure 3, with a given communication range R , node 3 is able to communicate with the reader between P1 and P2. Similarly, the reader can communicate with node 4 between P3 and P4.

The time for the reader to move from one end of the deployment to the other end of deployment, excluding the stop time for data collection, is a constant value depending on its moving velocity. Therefore, to minimize the communication delay of querying all sensor nodes, we just need to decide the optimal reader stop locations during its linear movement. Mathematically, we can have the following design objective:

$$\begin{aligned} \min \quad & \sum_{i=1}^{n_{stop}} T_i \\ \text{s.t.} \quad & \begin{cases} T_i = f(|S_i|) \\ \bigcup_{i=1}^{n_{stop}} S_i = S \end{cases} \end{aligned} \quad (1)$$

where n_{stop} refers to the total number of stops of reader, S_i denotes the set of nodes that the reader can communicate with at its i th stop, and the function $f(n)$ (i.e., delay curve) represents the communication delay with respect to the number of nodes within the communication range. Note that we need to jointly determine n_{stop} and their corresponding stop locations from infinity candidates on the linear track.

A. Design

Intuitively, if the reader can cover more nodes, we can reduce the number of stops. However, it increases contention in communication which leads to a longer delay during each stop. In this section, we balance the number of nodes reader can cover and the communication delay by transforming the delay minimization problem to a shortest path problem.

For a given deployment of n wireless rechargeable sensor nodes, we first sequentially index them as 1 to n based on their locations. This can be achieved based on RFID/WRSN localization methods after the deployment [19], [22]. Therefore,

given the communication range of a reader R , at any location, we can count the number of nodes the reader can communicate with. For the purpose of a clear explanation of the main concept of our proposed method, we assume a fixed isotropic communication range R of the reader in the rest of the paper. Although non-isotropic communication range has been studied in several papers, we claim that the simplification has little impact on our delay minimizing scenario in wireless rechargeable sensor networks. Measurement studies have shown that up to a certain distance from the sending nodes, the packet reception rates are uniformly high [30]. Since the charging range is relatively smaller than the communication range, the majority of nodes that can work properly have high-quality links with the reader. In addition, the estimation of the number of nodes can be achieved based on methods in modeling the non-isotropic communication range [33], e.g., through probabilistic ways. In Section V-C, we will further evaluate and discuss the impacts of the non-isotropic communication range.

Given the range R , at any location, the reader can communicate with a fixed number of nodes and there exists a finite numbers of communication states that the reader can communicate with different sets of nodes. For example in Figure 4(a), there are three wireless rechargeable sensor nodes and we index them 1 to 3 sequentially. As the reader moves from left to right, based on the communication range of the reader (shown as circles in Figure 4(a)), the reader first can communicate with node 1, then cover both node 1 and node 2, then node 2 alone, finally communicate with node 3. Consequently, there are four different communication states for the reader in Figure 4(a), namely $V_1 = \{1\}$, $V_2 = \{1, 2\}$, $V_3 = \{2\}$ and $V_4 = \{3\}$.

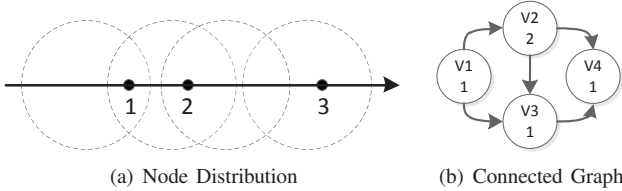


Figure 4. Example E_1 in Linear Dimension

After obtaining all communication states for the reader, we then construct a state connection graph based on the rules listed below to construct a graph:

States Connection Rules:

- State V_i connects to V_j if $V_i \cap V_j \neq \emptyset$
- State V_i connects to V_j if $\min(V_j) = \max(V_i) + 1$

where $\min(V_i)$ and $\max(V_i)$ denote the minimal node ID and the maximal node ID in a communication state V_i . Figure 4(b) shows the constructed graph. Essentially, the connection of two states denotes that the reader can communicate with a consecutive number of nodes without omitting any node in the middle. For example in Figure 4(a), $V_2 = \{1, 2\}$ connects to $V_3 = \{2\}$ because the reader can communicate with all nodes in the set $\{1, 2\}$. On the contrary, $V_1 = \{1\}$ does not connect to $V_4 = \{3\}$ since node 2 is omitted from the consecutive number set $\{1, 2, 3\}$.

After constructing the communication state graph, we then assign weights to individual vertices in the graph based on the

function $f(n)$ that represents the communication delay with respect to the number of nodes within the communication range of the reader. For each communication state V_i , we assign its weight to be $w_i = f(|V_i|)$. In Figure 4(b), we show an example of assigning weight to each vertex with delay function $f(|V_i|) = |V_i|$.

For the whole transformation process, it consists of scanning for communication states, graph construction and weight assignment. The computational complexity for this process is $\mathcal{O}(n)$, where n is the number of nodes in the network.

In the transformed graph, essentially each vertex represents one potential stop of the reader and the weight within each vertex represents the corresponding communication delay for the reader to finish communication at that stop. For each path from the first vertex to the last vertex in the graph, it represents one feasible solution for the reader to communicate with all nodes in the network. Therefore, to find the minimal communication delay with linear reader movement, we just need to find the shortest path from the first vertex to the last vertex in the transformed graph. Many existing algorithms [4] [12] can efficiently solve such shortest path problem in a graph with a complexity of $\mathcal{O}(V \lg V + E)$, where V is the cardinality of vertices and E is the cardinality of edges in a graph.

In some scenarios, multiple separate tracks have been pre-laid in places such as warehouses and readers move along these tracks to communicate with tags within dedicated areas. In such cases, delay minimization problem can be directly transformed into linear reader movement and well-solved by the algorithm introduced in this section. In the following section, we discuss a more generic solution where the reader can freely move in a two-dimensional space.

IV. MINIMIZING COMMUNICATION DELAY WITH TWO-DIMENSIONAL READER MOVEMENT

In a generic two-dimensional reader movement scenario, we assume the RFID reader can be carried by a vehicle or robot, and move to any location in a two-dimensional space [1]. Depending on the accuracy of localization and navigation of the vehicle/robot, we can divide the two-dimensional plane into $M \times M$ grids as shown in Figure 5, where each unit represents the minimal recognizable distance by the vehicle/robot.

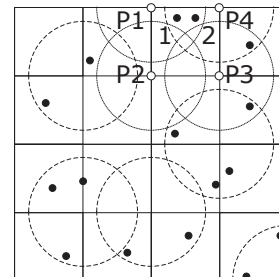


Figure 5. 2D Distribution of WISP Nodes

However in a two-dimensional space, we observe that we cannot solve Equation 1 within polynomial time and optimally plan the movement trajectory of the RFID reader as it is an NP-hard problem. So in this section, we first formally prove

the communication delay minimization problem in Equation 1 is NP-hard for the generic two-dimensional reader movement pattern and then propose an approximation solution with a provable approximation ratio.

A. NP-hard Proof

We reduce a known NP-hard problem, the weighted set-covering problem (WSCP) [13], to our communication delay minimization problem to prove its NP-hardness.

Definition of Weighted Set-Covering Problem: There is a finite set X and a family \mathcal{F} of subsets of X , such that every element of X belongs to at least one subset in \mathcal{F} : $X = \bigcup_{S \in \mathcal{F}} S$. Each set S_i in the family \mathcal{F} has an associated weight w_i . The weighted set-covering problem is to find a minimum-weight subset $\mathcal{C} \subseteq \mathcal{F}$ which covers all elements in X : $X = \bigcup_{S \in \mathcal{C}} S$.

The weight of a cover \mathcal{C} is $\sum_{S_i \in \mathcal{C}} w_i$.

For our delay minimization problem, let all nodes in the network form the set X . Then for each potential reader stop location i , the node that can communicate with the reader form the set S_i and its corresponding weight $w_i = f(|S_i|)$ where $|S_i|$ is the number of nodes within set S_i . Family \mathcal{F} consists of S and it is obvious to see that $X = \bigcup_{S \in \mathcal{F}} S$. To find the optimal reader stop locations, we need to find a set $\mathcal{C} \subseteq \mathcal{F}$ which has the minimum weight. Consequently, we reduce the WSCP to our delay minimization problem and prove the NP-hardness.

B. Approximation Solution

For WSCP, there exist several approximation solutions. In this work, we adopt a greedy-based algorithm *GA-2D* which has an approximation ratio $\rho_1 = H(\max\{|S|\} : S \in \mathcal{F})$ [10], where H represents harmonic series.

Algorithm 1 *GA-2D: Algorithm for 2D Delay Minimizing*

```

1: Input:  $X$  and  $\mathcal{F}$ 
2:  $U \leftarrow X$ 
3:  $\mathcal{C} \leftarrow \emptyset$ 
4: while  $U \neq \emptyset$  do
5:   select an  $S \in \mathcal{F}$  that minimize  $\frac{w_S}{S \cap U}$ 
6:    $U \leftarrow U - S$ 
7:    $\mathcal{C} \leftarrow \mathcal{C} \cup \{S\}$ 
8: end while
9: return  $\mathcal{C}$ 

```

As shown in Algorithm 1, based on the node set X and family \mathcal{F} , we firstly initialize system variables U and \mathcal{C} (Line 2 and Line 3). U refers to the set of uncovered nodes and equals to X initially. For each cycle in the loop, we find a set $S \in \mathcal{F}$, which has the $\min \frac{w_S}{S \cap U}$ (Line 5) firstly. It means that communication with nodes in S has the minimum average delay cost. Then nodes in S is removed from U (Line 6) since they have been successfully queried and set \mathcal{C} records such S in each selection attempt (Line 7). Algorithm ends until $U = \emptyset$. Since the reader could be continuously replied by nodes under multi-reply pattern, the sequence of reader stop locations will not affect the total communication delay. Therefore, given stop locations and durations, we can use any travel algorithm to

optimize the travel delay until algorithm *GA-2D* terminated. It is easy to prove the computation complexity of Algorithm 1 is $O(nM^2)$, where n is the number of sensor nodes.

V. DISCUSSION

In this section, we discuss practical issues such as how to guarantee the percentage of successful communications, as well as how to deal with single-reply pattern and non-isotropic communication range.

A. Guaranteeing the Ratio of Successful Communications

In Section III and Section IV, we have introduced solutions on how to decide reader's stop locations and the corresponding stop durations. However, since delay variances existed in the reader-tag communications, if the reader stays at its stop locations exactly according to the delay mapping function, some nodes may fail to communicate with the reader successfully. Consequently, it is critical to study how to extend the stop durations of the reader so as to achieve high quality of communications in the network.

Assuming the frame size is N and there are n nodes in the network, each node randomly chooses a slot in the frame to reply to the reader. Let Ψ_N^n denote the probability that there is no successful slot in the frame (i.e., all slots in the frame are either empty or have a collision). To calculate Ψ_N^n , we condition on the state of the first slot and use total probability Ψ_N^n as

$$1 - \Psi_N^n = \frac{\binom{n}{1}(N-1)^{(n-1)}}{N^n} + \frac{(N-1)^n}{N^n}(1 - \Psi_{N-1}^n) + \sum_{i=2}^{n-1} \frac{\binom{n}{i}(N-1)^{(n-i)}}{N^n}(1 - \Psi_{N-1}^{n-i}) \quad (2)$$

In Equation 2, the first part on the right of the equation refers to the probability that the first slot is a successful slot. Second part refers to the probability that the first slot is an empty slot and there exists at least one successful slot in following slots. The third part adds the probability that the first slot contains i nodes and at least one successful slot exists in following slots. Since the probability that there is no successful slot in a frame sized N with only one node equals 0, and no successful slot exists if $N = 1$ and $n > 1$, Ψ_N^n can be recursively computed with such initial values as $\Psi_N^0 = 1$, $\Psi_1^n = 1(n \neq 1)$ and $\Psi_N^1 = 0$.

Since the probability that n nodes allocated to one slot is binomially distributed [25], given frame size N and number of nodes n , the probability that k successful slots exists in the frame could be represented as:

$$p_N^n(k) = \frac{k! \binom{n}{k} \binom{N}{k} (N-k)^{(n-k)} \Psi_{N-k}^{n-k}}{N^n} \quad (3)$$

Consequently, under DFSA the probability of successfully finishing communication with n_s nodes within n_f frames could be iteratively calculated. For example, if the frame size is fixed to N , this probability can be written as:

$$P_n^{n_s}(n_f) = \sum_{i=0}^{n_s} p_N^n(i) P_{n-i}^{n_s-i}(n_f - 1) \quad (4)$$

where the initial probability $P_n^{n_s}(1) = p_N^n(n_s)$.

After obtaining the probability of successful communication with n_s nodes within n_f frames and optimal reader stop locations, the probability of successful reader-tag communications with a given number of nodes can be guaranteed by extending the reader stop duration based on Equation 4. For example, at the location where reader covers n nodes and $n_s \leq n$ nodes need to be queried with probability P_0 , the stop duration T_0 of the reader can be computed as $T_0 = N \cdot N_f$, where N refers to the fixed frame size and N_f is the minimum number of frames such that $P_n^{n_s}(n_f) \geq P_0$ (Eq. 4).

B. Dealing with Single-Reply Communication Pattern

In this subsection, we briefly discuss how to minimize communication delays under both linear reader movement and two-dimensional reader movement patterns for the single-reply communication.

1) *Linear Reader Movement*: For the linear reader movement, the solution in Section III-A is generally applicable for both multiple-reply pattern and single reply-pattern. The only difference for the single-reply pattern is that the first state connection rule needs to be removed as there is no node reply to the reader in different communication states.

2) *Two-dimensional Reader Movement*: Under two-dimensional reader movement, some nodes may be covered multiple times when the reader moves among different locations. Different from multiple-reply pattern where nodes always reply to the reader, in the single-reply pattern, nodes will stay in the silent state after a successful communications with the reader. Consequently, the communication delay for each reader stop locations is affected by the sequence of reader stop locations. Similar to the multiple-reply pattern, we prove the solution for single-reply pattern is also NP-hard. By utilizing the same heuristic algorithm in Section IV-B, we can have its approximation ratio under single-reply pattern as:

$$\rho_2 = \frac{\max\left(\frac{w_s}{|S|}\right)}{N \min\left(\frac{w_s}{|S|}\right)} \sum_{S \in \mathcal{F}} |S| H(\max\{|S|\} : S \in \mathcal{F}) \quad (5)$$

Detailed NP-hard proof and the derivation of ρ_2 are omitted due to the space constraint.

C. Non-isotropic Communication Range

We examine the impact of non-isotropic communication range in this section. DOI (Degree Of Irregularity) model in [33] is used as an example (see Figure 6(a)).

If the communication range of the reader is not circular shaped, reader may fail to communicate with some nodes within its communication range R . Thus the total communication delay may increase due to additional stops of the reader to cover these missed nodes. In this section, we empirically study the impact of the communication range irregularity, simulate the delays of two-dimensional reader movement in an $60m \times 60m$ area and compare the results of isotropic and non-isotropic communication range. The mapping function f we use is derived from experimental results.

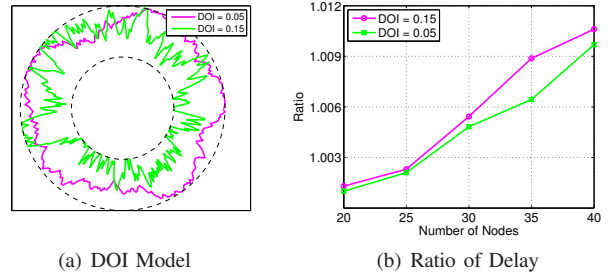


Figure 6. Delay with Non-isotropic Communication Range

Figure 6(b) shows the ratio of communication delay with isotropic and non-isotropic communication range, which reveals the impact of radio range irregularity on our proposed method. From Figure 6(b) we can see that the ratio of isotropic to non-isotropic communication range increases with DOI. However, the ratio remains very small when the number of nodes getting large with a high degree of irregularity (DOI = 0.15). This is due to the following two reasons. Firstly, since we set the center of the smallest enclosing disk of nodes as the stop location of the reader, average distance between nodes and the reader is minimized. Secondly, since the effective charging range is smaller than the communication range, during most stops of the reader, only a small number of nodes are covered in our proposed strategy according to the given f . Therefore they are more resilient to the irregularity of communication range. From Figure 6 we can safely make the conclusion that our proposed method is robust against irregular communication range and can be applied in scenario with non-isotropic communication model.

VI. EVALUATION

In order to understand the performance of proposed delay minimization algorithms under various settings, in this section we provide extensive simulations.

A. Simulation Setup

Except otherwise specified, RFID-based nodes with multiple-reply pattern are uniformly distributed in all scenarios. The minimal recognizable distance in the two-dimensional space is set to $1m$ and the reader communication range is set to $R = 10m$. As *a priori* knowledge, we define two mapping functions f_1 and f_2 between the number of nodes and the communication delay. Specially, f_1 is built based on the delay of DFSA with dynamic frame length that $f_1 = (0.1 + 0.05\lambda)n$ where λ is a 0.5-mean uniform distributed white noise with variance $\sigma = 1/12$. Furthermore, f_2 is obtained by simulation results of FSA with a fixed frame length. These two delay functions are chosen based on simulation results in Section II-C and theoretical results from [25].

In following sections, we compare our proposed algorithms with both the optimal delay and a baseline design. Specifically, we calculate optimal delays under two-dimensional movement through exhaustive search and in the baseline design, reader tries to cover maximal number of nodes which have not been queried during each of its stop.

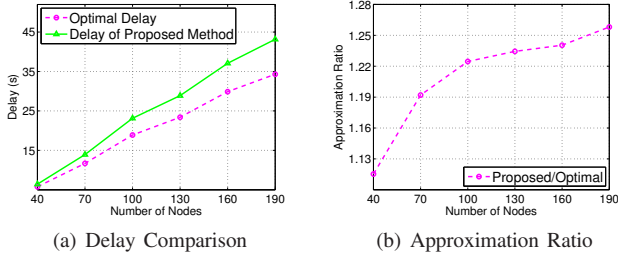


Figure 7. Delay with Two-dimensional Reader Movement

B. Performance of Two-dimensional Reader Movement

In Section III and Section IV, we propose delay minimization algorithms with linear reader movement and two-dimensional movement respectively. Since our design guarantees the optimal delay for the linear reader movement, in this section, we demonstrate the performance of our proposed approximation algorithm for two-dimensional reader movement. Specifically, 40 to 190 nodes are distributed in a $40m \times 40m$ area, and we compare the optimal delays of the two-dimensional reader movement with results of proposed design. The minimal recognizable distance is set to $10m$ and we adopt delay function f_1 for illustration. Figures for f_2 are omitted since they demonstrate similar results as f_1 .

In Figure 7(a) we see that communication delay increases with increasing number of nodes. This is because reader tends to cover more nodes in each stop when the number of nodes increases within a fixed area. In addition, from Figure 7(b) we can see that the approximation ratio between delay of our two-dimensional movement design and the optimal delay also increases but remains within a small gap. This result supports our theoretical analysis in Section IV.

C. Impact of System Settings

In this section, we examine impacts of various system settings with respect to the communication delay. We compare both our optimal delays with linear reader movement and the results of our two-dimensional movement algorithm with the baseline method. Both of delay mapping functions f_1 and f_2 are used in this section.

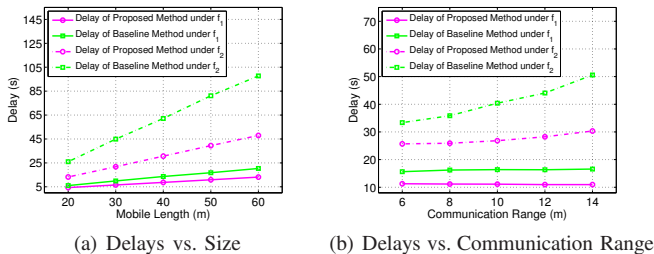


Figure 8. Impact of System Settings for Linear Movement

1) *Impact of Different Deployment Sizes:* Firstly we compare delays of different network deployment sizes with the same reader's communication range R . For linear reader movement, we set the length of track between $20m$ and $60m$. For two-dimensional reader movement, areas of regions in simulations are set to $60m \times 60m$ to $140m \times 140m$ with a

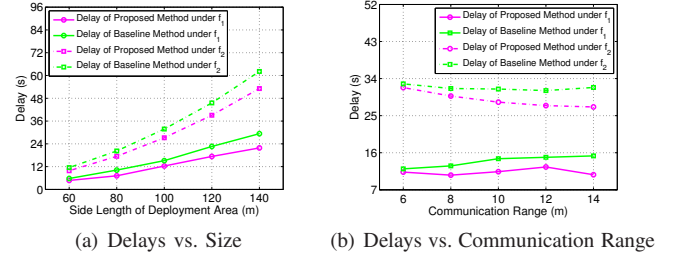


Figure 9. Impact of System Settings for Two-dimensional Movement

step length of $20m$. The communication delays of both types of reader movement are plotted in Figure 8(a) and Figure 9(a).

With fixed communication range R , reader may stop for multiple times to communicate with nodes deployed in a larger area. From both Figure 8(a) and Figure 9(a) we can see that communication delay increases linearly as deployment size getting larger. This is because of the uniform distribution of nodes and the result matches the analysis in Section II. By comparing delays under different mapping functions f_1 and f_2 , we can see our proposed methods outperform the heuristic method under all cases with at least 10% reduction in communication delay.

2) Impact of Different Reader Communication Ranges:

In this section, 100 nodes are deployed along a $100m$ -long track and in a $120m \times 120m$ area, respectively. In Figure 8(b) we can see delays of both algorithms under delay mapping function f_1 remain stable whereas under f_2 , both delays increase as communication range becomes larger. This is because the non-linear increase of f_2 leads to a much longer delay when more nodes can be covered at the same time. However, the delay of baseline method grows much faster than that of our proposed method under f_2 . From Figure 9(b) we can see that the communication delays of our proposed algorithms still exhibit better performances under both delay mapping functions with two-dimensional reader movement. For example, when communication range $R = 14$, the result of our proposed method has an improvement of 30% than the baseline method ($10.65s$ vs. $15.23s$).

D. System Performance under DFSA

In this section, we simulate communication dynamics and study the system performance under the widely implemented DFSA protocol [16]. Specifically, during the simulation, we set the size of first frame $N_1 = 2$ slots and increase the frame size based on the formula $N_i = 2.3922N_{i-1}^c$, where N_{i-1}^c refers to the number of collision slots in the previous frame [8].

Based on our design for linear reader movement, the ratio of successful communications refers to the ratio of average number of nodes with successful communication to the total number of nodes. In Figure 10, we can see that in most cases, ratio of successful communications is higher than 0.9 if the reader stops exactly as our design indicates. In other words, sensory data from more than 90% of nodes can be successfully retrieved. Furthermore, results for different stop durations are also presented in Figure 10. According to these results, we see that 10% increase of reader stop duration leads to approximately 4% increase of ratio of successful communications whereas a 10% reduction brings a 9% decrease of ratio of

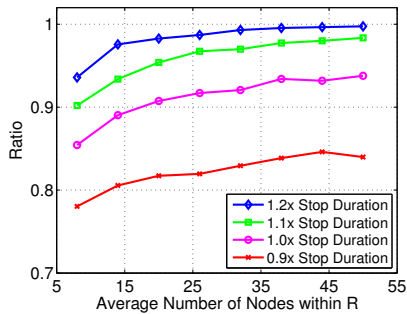


Figure 10. Ratio of Successfully Communicated Nodes

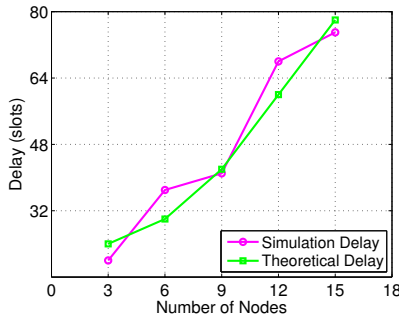


Figure 11. Comparison of Theoretical Delay and Simulated Delay

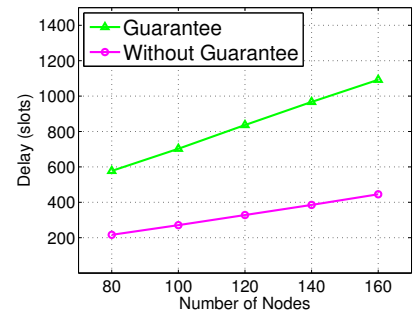


Figure 12. Communication Delay with Successful Communication Guarantee

successful communications. This result demonstrates a good balance between ratio of successful communications and delay.

E. The Effectiveness of Successful Communications Guarantee

In Section V-A, we introduce a design to achieve a higher quality of communication by extending stop durations. Here we set a fixed frame size $N = 6$ and validate the effectiveness of analytical results for successful communication guarantee in Section V-A.

1) *Model Validation*: In this section, we simulate communication process between the reader and multiple nodes for 1000 times to calculate the probability of successful communication when all nodes are covered by the reader. Specifically, we compare delays that all nodes successfully communicated with the reader in 95% runs with analytical results based on Equation 4 in Section V-A. From Figure 11, we can see the simulated delay matches our analytical result well. For example, when the number of nodes is 9, the difference of two delays is only one slot.

Table II. PROBABILITY P OF SUCCESSFUL COMMUNICATION OF ALL NODES

Number of Nodes	80	100	120	140	160
P with Guarantee	95.1%	96.4%	97.0%	97.8%	97.6%

2) *System Performance with Successful Communication Guarantee*: Based on the analytical result, the reader can extend its stop duration to achieve a higher successful communication ratio. In this section, we place 80 to 160 nodes in a $100m \times 100m$ area. The requirement of successful ratio of communication for all nodes is set to $P_0 = 95\%$ and we extend stop durations based on Equation 4 in Section V-A. Simulation results are shown in Table II and Figure 12.

From Table II, we can see that the actual ratio of successful communication of all nodes meets the system specifications, i.e., 95%. Figure 12 shows the corresponding communication delay under the 95% successful communication requirement. From this figure we can see that communication delay is tripled when the probability of successful communication with all nodes reaches 95%. Consider the percentage of successfully communicated nodes in Figure 10, we can see reader spend much more time to guarantee a high ratio of successful communication with all nodes in vicinity.

VII. RELATED WORK

Communication delay minimizing have been extensively studied in multi-hop wireless sensor networks [9], [18]. However in rechargeable environments, the majority of existing works focus on network utility optimization through energy management [15], [24], [27]. Due to the potential dense deployment and unique characteristics (e.g., relatively small charging delay) of RFID-based wireless rechargeable sensors, study on the communication delay minimizing is equally important.

As a representing wireless rechargeable sensor node, Wireless Identification and Sensing Platform (WISP) was firstly proposed by Intel Lab Seattle to enhance the functionalities of current RFID tags [20]. WISP has the capabilities of RFID tags, but also supports sensing and computing. Since then there have been many new works on applications as well as improvements of WISPs [26]. In [14], Gummeson et al. propose SolarWISPs that enhance original WISP's communication range, read rate and uptime in RAM retention mode with a micro solar panel. Buettner et al. implement a daily activity recognition application by integrating everyday objects (e.g., glass, plate, books) with WISP tags [6]. However, this line of work is mostly related to the hardware design and sustainable operation of individual nodes, but does not consider how to retrieve sensory data from multiple nodes with minimized communication delay and high reliability.

In traditional RFID systems, the communication delay minimization designs are mainly focused on the collision avoidance among RFID tags. Two primary strategies of anti-collision algorithms in RFID systems are slotted ALOHA based protocols [11] and tree based protocols [32]. In slotted ALOHA protocols, a tag probabilistically replies to the reader and will randomly retransmit if it collides with other tags. The Framed Slotted ALOHA protocol further groups several slots into frames and each tag randomly chooses a slot within the frame to reply once. Collision avoidance algorithms in slotted ALOHA have appeared in [16] [25] [31]. Kodialam et al. [16] propose a set of solutions including collision-based estimator and the probabilistic estimators for tag number estimation. Zhen et al. [31] adopt a continuous-time model and compute that the time used for reading N tags with a minimized probability of unsuccessful communication with a particular tag is $18.76N$. In [25], Vogt derives the time required to identify all tags with an assurance level α by modeling the reading process as a Markov process.

As deterministic identification algorithms, tree algorithms split the group of tags into subgroups by detecting collisions until all tags in each subgroup are identified. Examples of such algorithms can be found in [7] [8]. Although these algorithms deterministically resolve communication collisions, they often exclude time readers spend in sub-dividing nodes. Besides, they incur high computational overhead and long delay thus become less feasible with large scale deployment of RFID tags.

Different from existing works, in this work we introduce orthogonal and protocol-independent solutions that exploit fundamental relationship between reader-tag communication delay and the number of wireless rechargeable sensor nodes even under potential collisions. We expect our solutions can be generically applied to most existing RFID communication protocols and will also benefit from future improvements of these protocols.

VIII. CONCLUSION

In this paper, we study the problem of how to optimally plan the movement pattern of the RFID reader so as to minimize communication delay in RFID-based wireless rechargeable sensor networks. We first identify the fundamental relationship between the communication delay and the number of wireless rechargeable sensor nodes through mathematical analysis and empirical experiments. Based on this observation, we introduce an optimal solution for the linear reader movement pattern, as well as heuristic solutions with provable approximation ratio when a reader can freely move in a two-dimensional space. In addition, we also study practical issues such as how to guarantee the successful communication ratio in the network. To verify our designs, we perform detailed performance evaluations via thorough analysis, emulation and simulations. To the best of our knowledge, this is the first try in minimizing communication delay in RFID-based wireless rechargeable sensor networks and complementary to the advancement of existing RFID communication protocols.

ACKNOWLEDGMENT

The paper was partially supported by NSFC under Grant 61222305, National Program for Special Support of Top-Notch Young Professionals, Fundamental Research Funds for the Central Universities under Grant 2014XZZX001-03, 2014XZZX003-25, ZJNSF under Grant Y14F030048 and Grant SUTD-ZJU/RES/03/2011.

REFERENCES

- [1] Diakinisis Automates Major Distribution Center with RFID. http://www.aliantechnology.com/docs/CS_Diakinisis.pdf.
- [2] European Retailer Throttleman Improves Supply Chain with RFID. http://www.aliantechnology.com/docs/CS_Throttleman.pdf.
- [3] RFID for Passive Asset Tracking. <http://www.aliantechnology.com/docs/applications/SBAssetTracking.pdf>.
- [4] M. Barbehenn. A note on the complexity of dijkstra's algorithm for graphs with weighted vertices. *IEEE Trans. on Comput.*, 47(2):263, 1998.
- [5] D. J. Bijwaard, W. A. van Kleunen, P. J. Havinga, L. Kleiboer, and M. J. Bijl. Industry: Using Dynamic WSNs in Smart Logistics for Fruits and Pharmacy. In *ACM SenSys*, 2011.
- [6] M. Buettner, R. Prasad, M. Philipose, and D. Wetherall. Recognizing Daily Activities with RFID-based Sensors. In *ACM UbiComp*, 2009.

- [7] J. Capetanakis. Tree Algorithms for Packet Broadcast Channels. *IEEE Transactions on Information Theory*, 25(5):505 – 515, 1979.
- [8] J.-R. Cha and J.-H. Kim. Novel Anti-collision Algorithms for Fast Object Identification in RFID System. In *IEEE ICPADS*, 2005.
- [9] M. Cheng, Q. Ye, and L. Cai. Cross-Layer Schemes for Reducing Delay in Multihop Wireless Networks. *IEEE Transactions on Wireless Communications*, 12(2):928–937, 2013.
- [10] V. Chvatal. A Greedy Heuristic for the Set-covering Problem. *Mathematics of Operations Research*, 4(3):233–235, 1979.
- [11] EPCglobal. EPC Radio-Frequency Identity Protocols Class-1 Generation-2 UHF RFID Protocol for Communications at 860 MHz - 960 MHz Version 1.0.9, 2005.
- [12] L. Fu, D. Sun, and L. R. Rilett. Heuristic Shortest Path Algorithms for Transportation Applications: State of the Art. *Elsevier Computers & OR*, 33(11):3324–3343, 2006.
- [13] G. Gambosi, M. Protasi, and M. Talamo. Preserving Approximation in the Min-Weighted Set Cover Problem. *Discrete Applied Mathematics*, 73(1):13–22, 1997.
- [14] J. Gummeson, S. S. Clark, K. Fu, and D. Ganesan. On the Limits of Effective Hybrid Micro-energy Harvesting on Mobile CRFID Sensors. In *ACM MobiSys*, 2010.
- [15] S. He, J. Chen, F. Jiang, D. Yau, G. Xing, and Y. Sun. Energy provisioning in wireless rechargeable sensor networks. *IEEE Transactions on Mobile Computing*, 12(10):1931–1942, Oct 2013.
- [16] M. S. Kodialam and T. Nandagopal. Fast and Reliable Estimation Schemes in RFID Systems. In *ACM Mobicom*, 2006.
- [17] C.-H. Lee and C.-W. Chung. Efficient Storage Scheme and Query Processing for Supply Chain Management Using RFID. In *ACM SIGMOD*, 2008.
- [18] H. Li, X. Liu, W. He, J. Li, and W. Dou. End-to-end delay analysis in wireless network coding: A network calculus-based approach. In *IEEE ICDCS*, 2011.
- [19] L. Ni, D. Zhang, and M. Souryal. RFID-based Localization and Tracking Technologies. *IEEE Wireless Commun.*, 18(2):45–51, 2011.
- [20] A. P. Sample, D. J. Yeager, P. S. Powlledge, A. V. Mamishev, and J. R. Smith. Design of an RFID-Based Battery-Free Programmable Sensing Platform. *IEEE T. Instrum. Meas.*, 57(11):2608–2615, 2008.
- [21] F. Schoute. Dynamic Frame Length ALOHA. *IEEE Transactions on Communications*, 31(4):565–568, Apr 1983.
- [22] Y. Shu, P. Cheng, Y. Gu, J. Chen, and T. He. TOC: localizing wireless rechargeable sensors with time of charge. In *IEEE INFOCOM*, 2014.
- [23] Y. Shu, Y. J. Gu, and J. Chen. Dynamic authentication with sensory information for the access control systems. *IEEE Trans. Parallel Distrib. Syst.*, 25(2):427–436, 2014.
- [24] B. Tong, Z. Li, G. Wang, and W. Zhang. How wireless power charging technology affects sensor network deployment and routing. In *IEEE ICDCS*, 2010.
- [25] H. Vogt. Efficient Object Identification with Passive RFID Tags. In *Pervasive*, pages 98–113, 2002.
- [26] First workshop on Wirelessly Powered Sensor Networks and Computational RFID. <http://seattle.intel-research.net/wisp/summit/>.
- [27] L. Xie, Y. Shi, Y. T. Hou, and H. D. Sherali. Making sensor networks immortal: an energy-renewal approach with wireless power transfer. *IEEE/ACM Trans. Netw.*, 20(6):1748–1761, 2012.
- [28] G. Xing, T. Wang, W. Jia, and M. Li. Rendezvous Design Algorithms for Wireless Sensor Networks with a Mobile Base Station. In *ACM Mobicom*, 2008.
- [29] X. Xu, L. Gu, J. Wang, and G. Xing. Negotiate Power and Performance in the Reality of RFID Systems. In *IEEE PerCom*, 2010.
- [30] J. Zhao and R. Govindan. Understanding packet delivery performance in dense wireless sensor networks. In *ACM SenSys*, 2003.
- [31] B. Zhen, M. Kobayashi, and M. Shimizu. To Read Transmitter-only RFID Tags with Confidence. In *IEEE PIMRC*, 2004.
- [32] Y. Zheng, M. Li, and C. Qian. PET: Probabilistic Estimating Tree for Large-Scale RFID Estimation. In *IEEE ICDCS*, 2011.
- [33] G. Zhou, T. He, S. Krishnamurthy, and J. A. Stankovic. Impact of Radio Irregularity on Wireless Sensor Networks. In *ACM MobiSys*, 2004.